Chapter 15
Spatial-Temporal Quantification of Interdependencies Across Infrastructure Networks

Christopher Chan and Leonardo Dueñas-Osorio

Abstract As infrastructure networks become more complex and intertwined, the relevance of network interdependency research is increasingly evident. Interconnected networks bring about efficiencies during normal operations but also come with risks of cascading failures with disaster events. An adequate understanding of network interdependencies and realistic multi-system modeling capabilities enable the exploration of practical operation strategies and mitigation efforts applicable to existing or future coupled networked systems. This chapter examines recent efforts in quantifying infrastructure network interdependencies through spatial and time-series analyses to reveal the heterogeneity and complexity in their coupling. Furthermore, a combined spatial-temporal methodology is recommended for the future calibration and validation of theoretical and computational models of interdependent networks of networks. An example case study is demonstrated using data derived from the 2010 Chilean Earthquake in the Talcahuano-Concepción region, which highlights the richness in coupling strengths across infrastructure systems, both as a function of time and geographical extent. Insights for design and control of coupled networks are also derivable from joint spatial-temporal analyses of infrastructure interdependence and its evolution.

15.1 Introduction

From the World Wide Web to the national power grid, networks are an essential part of the world. Appearing in almost all aspects of modern society, a network connects individual components, or nodes, with links that join together multiple

C. Chan (✉)
Stanford University, 450 Serra Mall, Stanford, USA
e-mail: chris.chan@stanford.edu

L. Dueñas-Osorio
Rice University, 6100 Main Street, Houston, USA
e-mail: leonardo.duenas-osorio@rice.edu

G. D'Agostino and A. Scala (eds.), *Networks of Networks: The Last Frontier of Complexity*, Understanding Complex Systems, DOI: 10.1007/978-3-319-03518-5_15,

nodes in a systemized network. Common networks include public transportation systems, electrical power grids, water systems, and intertwined social circles [14, 18]—examples that are frequently seen in everyday life. Hence, a more complex network can be defined as the coupled interaction of those individual networks with each other; for example, much of a city's service infrastructures, like the water supply network and subway systems, are dependent upon the greater regional power network, which may be contingent upon functioning telecommunications channels which govern the operations of a series of other networks and infrastructure systems [22, 34]. Similarly in fields differing from engineering, biochemically linked neurons in the body work both synchronously and in tandem with the other biological systems to sustain even greater functions [2, 4]. These interdependencies between networks create a complex web of networks of networks linked by both connectivity and dependency [13, 17, 29], which significantly increases efficiency, but also introduces greater risks in network security and reliability.

Network interdependency has especial relevance within infrastructure systems. As the world continues to urbanize, essential infrastructures have become increasingly interconnected and mutually dependent with new tech0nological advances [3, 13, 34]. Any disruption with critical infrastructure can result in what is known as cascading failures [6, 15, 36, 42] in which one failure causes a chain event result. On July 30 and 31 of 2012, more than 700 million people, roughly a tenth of the world's population, were plunged into darkness in northern India, as the three interdependent state power grids crippled one after the other [20]. The world's largest blackout paralyzed the interstate train system, affected local health services, and trapped 200 miners among other consequences [39]. The magnitude of the incident lucidly demonstrated the criticality of linked networks and manifested the extent that interdependent infrastructures can impact the world.

The inherent nature of increasingly connected and interdependent infrastructure systems implies that there will continue to be even greater risks and vulnerabilities during operations as well as even more pronounced repercussions in the event of external threats. Such dangers ranging from natural disasters to terrorist attacks can put the connected network of networks at risk of a falling domino effect. In fact, the reliability of critical infrastructure security became such an issue in the United States that in 1996 President Clinton issued an executive order to establish the President's Commission on Critical Infrastructure Protection (PCCIP) [8, 21, 30]. The importance of critical infrastructures means that it is necessary to not only model the complexities of infrastructure networks, but also quantify the inherent risk associated with interdependency.

As a result, much of recent research in the past decade has been devoted to examining and understanding infrastructure network interdependencies [34]. This can be done through a host of strategies, for example, identifying the mechanisms of interaction (physical, logistical, geographical, etc.), observing the interdependent characteristics (operational, spatial, temporal, etc.), and quantifying the coupling and response behaviors [24, 32]. This chapter will look at research and models to quantify the interdependencies of infrastructure networks and infer their potential effects on system performance. Models and simulations in the past have employed a variety

of techniques to measure and capture the complex interactions in interdependent networks with a mixture of approaches deriving from complexity and network theories, economic methods, probabilistic analyses, and data-driven approaches. For example, frequency analyses of infrastructure failure propagation incidents after hazards have been studied as a methodology for characterizing and empirically quantifying network interdependencies [7, 26]. From theoretical and simulation-based approaches, sandpile dynamics have been used with a multi-type branching process to analyze cascading loads in connected networks of different topologies [5]. With the increase in computing power, complex adaptive systems (CAS) have also been used to model interdependent networks as individual intelligent agents which cooperate and compete in the larger system. The agent-based CAS modeling could use sensors in the system to prevent cascading failures and is applied frequently among operational and socioeconomic networks [1]. Borrowing off of financial markets modeling, the Leontief economic paradigm, when applied to infrastructure networks, is an input–output model that uses an interdependence matrix to compute shared risk of inoperability of infrastructure systems [21]. Restoration of network services has also been modeled using multilevel interdependencies in a mathematical network flows model exploiting advances in operations research [25], while computationally intensive, flow dynamic-based methods that require large data sets have been applied to models of telecommunications, gas, power, and emergency systems [28, 33, 35]. In addition, the graph wavelets approach, which uses the wavelet transform to model changes in the network as a whole, has been used in spatial traffic flow analysis, which has the potential to impact multiple physical and social systems [10]. Finally, network reliability models that use a probabilistic quantification of interdependencies among networks provide flexibility to integrate with network theory and quantify performance correlations between infrastructure systems which provide unique insights for infrastructure engineering practice [23].

While these and many other approaches to modeling interdependent systems exist, for any method, the quantification of coupling, calibration of performance assessment models, and verification of predictions in a sundry of scenarios remains vital to research and practical applications in network interdependency. Recent approaches have utilized time-based analyses of multi-network performance to calculate coupling strengths by using temporal correlations of post-disruption restoration times [16]. At the same time, network interdependency can also be approached by looking at spatial correlation. Studies have taken stochastic external stresses to identify geographic vulnerabilities [31] or utilized kriging techniques in generating spatial correlation [40]. The methodology presented in this chapter allows for a novel approach to quantify joint spatial-temporal network correlations and reveals the heterogeneity in the interdependencies of infrastructure systems that simultaneously take into account the time-dependent and geographic relevance of the networks.

The following sections will briefly overview approaches that have been used to quantify interdependence, specifically with regard to time- and space-dependent methods and, furthermore, describe the unique spatial-temporal approach recommended by this study. After the methodological discussions, this chapter will focus on the application of the spatial-temporal approach to representations of data derived

from post-event analysis of the 2010 moment magnitude (M_W) 8.8 Chilean earthquake, and finally, the analysis of results and synthesis of insights will be followed by conclusions and suggestions for future work on interdependent infrastructure networks research.

15.2 Methodological Approaches to Quantifying Network Interdependencies

15.2.1 Temporal Methodologies

In order to quantify interdependencies across networks and enable the calibration of models of networks of networks, recent studies have taken a time-series approach in analyzing coupling strengths between infrastructure networks. Dueñas-Osorio and Kwasinski [16] explore such an approach by looking at utility service restoration responses. Utilizing post-disaster restoration information from the 2010 Chilean Earthquake, data from individual utility service systems, or lifeline system restoration curves, were collected, showing the gradual restoration of power, water, and telecommunication services available as a function of time. Auto-covariance and autocorrelations of the restoration data were calculated to assess temporal dependencies within the same system. To measure the coupling strength between different utility networks, the cross-correlation $\rho_{j,k}$ (Eq. 15.2) was calculated using the cross-covariances $\gamma_{j,k}$ (Eq. 15.1) for given time lags (or relative times between the restoration curves) using the following equations:

$$\gamma_{j,k}(h) = \frac{1}{1+n_j} \sum_{t=0}^{n_j-h} (x_{t+h,j} \bar{x}_j)(x_{t,k} - \bar{x}_k), \tag{15.1}$$

$$\rho_{j,k}(h) = \frac{\gamma_{j,k}(h)}{\sqrt{\gamma_j(0)\gamma_k(0)}}, \tag{15.2}$$

where $x_{t,j}$ or $x_{t,k}$ is the restoration value at time t of the jth or kth system, n_j is the maximum observation time, and h is the given time lag between the restoration curves of the systems. The cross-correlations provide a convenient dimensionless metric for quantifying interdependencies and analyzing the behavior of the systems across the restoration time series, and in this way, leading or lagging interdependence properties of the networks can be revealed. In order to achieve stationarity and make the time-series analysis tools suitable, the time-series data is transformed and second-differenced before the correlation analysis. The study notes high correlations between power and telecommunications systems (operational interdependency) as well as with water delivery (logistical interdependency). For example, correlation between fixed phone services and the regional power delivery system reaches 0.84 at a lag time of $h = 2$, highlighting the high level of operational interdependency

between power and telecommunications with the latter lagging in restoration. Similarly, strong correlation between power and water systems reaches 0.79, but at a negative lag time of $h = -13$, showing the leading tendency of the power system restoration on the ability of water system operators to coordinate the logistics of damage repairs. Outcomes are only observed several days later after intensive physical tasks of digging, welding, and replacing are completed. A mathematical relationship is then formulated as a measure of overall coupling strength $S_{j,k}$ (Eq. 15.3), reflecting both the time lag and the system correlations and demonstrates a high level of interdependence among power and telecommunication systems in regions with moderate level of damage, as well as strong intra-dependence within systems of the same type. In addition, the study reveals a high degree of infrastructure coupling between neighboring regions where the leading restoration of power and telecommunication systems directly affects closely linked restoration processes of networks in geographically close regions.

$$S_{j,k} = \begin{cases} -\rho_{j,k}(h)/(1+\sqrt{|h|}) & \text{when } h \neq 0 \\ \rho_{j,k}(h) & \text{when } h = 0 \end{cases} \tag{15.3}$$

Using a time-series post-event interdependence quantification technique and analyzing the autocorrelations and cross-correlations in restoration data across systems, it is possible to not only capture the holistic operational and logistical coupling between two networks after a critical failure, but also identify leading and lagging relationships to improve performance and adopt effective mitigation actions for interdependent systems. The quantification of coupling strengths allows for potential applications in computational and theoretical predictive models as well as in disaster mitigation efforts for infrastructure operations and recovery. In the end, practical applications of quantified coupling strengths can include the exploration of system decentralization or the uncoupling of systems during emergency operations to enhance restoration as well as identification of specific physical or organizational factors affecting restoration rates.

15.2.2 Spatial Methodologies

Another significant dimension in quantifying interdependency, especially for infrastructure systems, is the geographic correlation between network elements and their performance. Spatial proximity among networks holds important relevance in modeling infrastructure interdependencies, most notably in the aftermath of natural disasters, such as earthquakes as demonstrated by Lee and Kiremidjian [27] and Rahnamay-Naeini et al. [31]. In modeling spatially-dependent systems, geostatistical techniques like ordinary point kriging utilize optimal least-squares predictions and can be employed in a probabilistic analysis of infrastructure networks to quantify their interdependencies as distributed in their service area spaces. Wu et al. [40] demonstrate the application of kriging surfaces on utility restoration records and

the calculation of spatial correlations to estimate the spatial distribution of network interdependencies among the lifeline systems of Sect. 15.2.1.

15.2.2.1 Ordinary Point Kriging

Ordinary point kriging is a geostatistical technique recently embraced by the spatial interdependence assessment methodology as a tool for spatial interpolation in the creation of restoration and correlation surfaces. Specific details are further discussed below as they are central to the formulation of the spatial-temporal approach proposed in Sect. 15.2.3 of this chapter.

In the analysis of spatial interdependency, a spatial surface of the infrastructure system parameter (e.g. service restoration) must be created by kriging using the mesh of original evaluation data points. With ordinary point kriging, interpolation of restoration records and their spatial variability necessitates an estimator variogram γ_E (sometimes refered to as a 'semi-variogram' governed by Eq. 15.4). The estimated variogram enables plotting spatial variation versus distance, and a parametric curve can then be fitted to model the spatial data [38]. Commonly used parametric models include the spherical, exponential, and linear models, etc.

$$\gamma_E(d) = \frac{1}{2N(d)} \sum_{i=1}^{N(d)} (z_{x_i} - z_{x_i+d})^2 \,, \tag{15.4}$$

In defining $\gamma_E(d)$, z_{x_i} and z_{x_i+d} are the restoration values at the evaluation points x_i and $x_i + d$, respectively. $N(d)$ is the cardinality of the set of pairs of points within a spatial lag or relative distance of d, and the lag interval d is defined as the Euclidian distance between points x_i and $x_i + d$, where the maximum lag is often set as the mean minimum distance between a given pair in the data set. Using a parametrically fitted variogram model (exponential, in the Chilean data case), the restoration values are then interpolated in a mesh grid by ordinary point kriging, which uses a weighted average of the other neighboring evaluation nodes with weight coefficients λ_i that are estimated by minimizing the mean-square error, or kriging variance, and satisfy the following constraints:

$$\hat{z}_p = \sum_{i=1}^{N} (\lambda_i z_{p_i}) \tag{15.5}$$

$$\sum_{i=1}^{N} (\lambda_i) = 1 \tag{15.6}$$

$$E(\hat{z}_p - z_p) = 0 \tag{15.7}$$

$$E((\hat{z}_p - z_p)^2) = 2 \sum_{i=1}^{N} \lambda_i \gamma(x_i, x_p) - \sum_{i=1}^{N} \sum_{j=1}^{N} \lambda_i \lambda_j \gamma(x_i, x_j) \tag{15.8}$$

where $E(\square)$ is the minimized estimation, N is the number of neighboring evaluation points, z_{p_i}, in the context of infrastructure systems after disruption, is the restoration level at a particular point of interest x_i, while $\hat{z}_p$ and z_p are the estimated interpolated value and true restoration value at the interpolation point of interest p respectively. The function $\gamma(x_i, x_p)$ provides the variogram value between the evaluation point at x_i and the particular point x_p, and $\gamma(x_i, x_j)$ is the variogram value associated with neighboring evaluation points x_i and x_j. Spatial interdependence between the two systems is calculated using cross-correlations among the stationary z_{pi} restoration values at the location of evaluation points x_i of a particular network (known as the reference network) and those of a second network (known as the adjuct network) while using a neighborhood set of $\hat{z}_p$ values around the evaluation points x_i of one system and the corresponding set of zp_{hat} values that are collocated in the other system to establish local interdependence strengths as a function of geographical location. Such interdependence strengths are finally used to create a kriging-based surface of local interdependence across systems, which is heterogeneous in contrast to typically assumed constant values of coupling strengths for all interdependence links.

15.2.2.2 Spatial Applications to Chilean Data

An application of spatial kriging techniques is performed on the post-disaster Chilean data in Wu et al. [40]. Cross-correlation of geographically distributed service restoration times for water and power networks are used first as a proxy for spatial interdependency quantification and mapping of local coupling heterogeneity into correlation surfaces. Then, correlation values across systems are synthesized as a function of relative angle and radial distance between restoration surfaces away from one of the system's set of evaluation nodes. Specifically, by shifting the adjunct system's kriging restoration surface from the surface of the reference system and calculating the correlation values, the spatial interdependency of the two systems can be found by the different cross-correlation and autocorrelation values, the latter being that in which the same network serves as both the reference and adjunct network. Such synthesized correlations are quantified using Pearson's coefficient (a measure of linear correlation) as well as Kendall's tau coefficient (rank correlation). The resulting data is plotted on polar coordinates to represent spatial interdependencies from a suite of relative angles and distances across restoration surfaces, forming global correlation plots. These plots demonstrate certain patterns in the analysis, specifically in the cross-correlation between power as the reference system and water as the adjunct system, where a southwest to northeast spatial directionality of the interdependence is evident, revealing spatial coincidence in the average restoration time trends along the noted geographical corridor, partially due to the topology of the systems and the patterns of damage. (Additional details are provided in Sect. 15.4 regarding directionality trends in spatial interdependencies.) Overall correlation plots are then created by averaging the global correlations across all angles, resulting in initial cross-correlation values as a function of relative distance between

restoration surfaces of 0.483 and 0.284 for Pearson's coefficient and Kendall's tau coefficient, respectively. The average correlation plots also reveal certain characteristics of interdependence, such as the average distance away from evaluation nodes until correlation values become negligible or reach zero, which can be interpreted as a measure for spatial coupling strength decay or interdependence length [40]. These interdependence lengths can readily inform utility operators about optimal system decoupling schemes as well as requirements for temporary back-up systems, given that the reach of interdependence is spatially confined to manageable distances.

15.2.3 Spatial-Temporal Methods

Both the time-series model and the spatial methods offer unique insights into the true nature of interdependent infrastructure networks, but emerging strategies in estimation and modeling of networks of networks attempt to encompass more realistic constraints, as when having both correlations in a single spatial-temporal model. By assessing the appropriateness of a series of assumptions regarding the covariance structure across systems in time and space, including full symmetry, separability and stationarity, a number of methodologies have been proposed that have wide ranging practical applications [19].

In order to combine spatial covariances (or variograms) with temporal ones, a variety of models are available, some of which are suitable for novel applications in infrastructure interdependency assessment problems. In order to be a valid covariance function, the combined variogram must satisfy the condition of positive definiteness, where a matrix remains nonnegative definite for all combinations of space-time coordinates [11, 19]. The Product Model separates temporal and spatial considerations and disregards dependence between space and time covariance, but offers a simple and efficient way to represent a spatial-temporal covariance. The Linear Model simply separates and sums up the two covariances, resulting in only a positive semi-definite function [11]. The simplicity of the Product Model and the Linear Model are often inapplicable to certain real world examples due to their inherent assumptions on separability and positive definiteness. As a result, Cressie and Huang derived a new approach to tackle nonseparable stationary covariance functions. By utilizing Bochner's Theorem and assuming integrability, positive definiteness can be proved using the Fourier transform on the spectral density, thereby creating a class of stationary spatial-temporal covariance functions [9]. However, the complexity of the Cressie and Huang model motivated the development of a more flexible and general Product-Sum Model which combines the simplicity of the product and linear models with the applicability that satisfies the conditions of a viable covariance function. The Product-Sum model enables, for the first time, the practical quantification of interdependencies in time and space and provides a reference for models of networks of networks to use in terms of their necessary input coupling information.

15.2.3.1 The Product-Sum Model

De Cesare et al. [11] promotes a Product-Sum model that, as its name suggests, serves as a simple hybrid between the Linear and Product models in the past. De Iaco [12] further refines a generalized version of the Product-Sum model and explores in depth how to fit data to the spatial-temporal variogram. The practical model introduced to represent spatial-temporal covariances is as follows:

$$Cov_{st}(h_s, h_t) = k_1 Cov_s(h_s) Cov_t(h_t) + k_2 Cov_s(h_s) + k_3 Cov_t(h_t), \tag{15.9}$$

where Cov_s and Cov_t represent the separate spatial and temporal covariance models respectively, h is the generic lag, which is qualified by the subindices s and t for spatial and temporal, and k_1, k_2, and k_3 are constants determined by the individual variogram sills, defined as the plateauing γ limit of the variogram approximating the population variance [38]. The equivalent combined function using variograms is as follows:

$$\gamma_{s,t}(h_s, h_t) = (k_2 + k_1 C_t(0))\gamma_s(h_s) + (k_3 + k_1 C_s(0))\gamma_t(h_t) - k_1 \gamma_s(h_s)\gamma_t(h_t), \tag{15.10}$$

where $\gamma_{s,t}$ represents the spatial-temporal variogram and γ_s and γ_t are the respective spatial and temporal variogram models. In addition, C_s, C_t, and C_{st} are the sills, estimated from the parametric curve corresponding to each bounded variogram. Each variogram is found by the following general equation, where $\gamma_s(h_s) = \gamma_{s,t}(h_s, h_t = 0)$ and $\gamma_s(h_t) = \gamma_{s,t}(h_s = 0, h_t)$:

$$\gamma_{s,t}(h_s, h_t) = \frac{Var(Z(s + h_s, t + h_t), Z(s, t))}{2}, \tag{15.11}$$

where Z is a second order stationary spatial-temporal random field of the restoration levels and s, t are space and time values in the respective domains. By using the sills to calculate the three coefficients, positive definiteness can be guaranteed when $k_1 > 0, k_2 \geq 0$ and $k_3 \geq 0$, and the following expressions are used:

$$k_1 = [C_s(0) + C_t(0) - C_{st}(0, 0)]/C_s(0)C_t(0) \tag{15.12}$$

$$k_2 = [C_{st}(0, 0) - C_t(0)]/C_s(0) \tag{15.13}$$

$$k_3 = [C_{st}(0, 0) - C_s(0)]/C_t(0)\ . \tag{15.14}$$

Spatial-temporal methods already have widespread applications across environmental monitoring and modeling, ranging from air pollution to wind speed monitoring, but the concepts can be adopted and customized to infrastructure network models as well. This chapter demonstrates next the relevance of the Product-Sum method to representations of both temporal and spatial data derived from utility restoration processes after the 2010 M_W 8.8 Chile Earthquake.

15.3 Application of the Spatial-Temporal Methodology to the 2010 Chilean Earthquake

The introduced spatial-temporal methodology is applied onto representations of lifeline systems restoration data throughout time and space derived from field-collected nodal values after the 2010 Chilean Earthquake [37]. A total of 93 evaluation nodes covering the service area of two infrastructure networks are used in the study, shown on the map in Fig. 15.1. The level of restoration at each of the evaluation nodes is represented as the percent of fully restored services provided by each of the power and water lifeline networks, which reflects both the level of damage inflicted on the node as well as the prioritization of the post-event restoration procedure. The temporal data at each node is assumed to follow the shape of restoration curves found in the local power and water delivery networks in the Talcahuano and Concepción region [16].

The joint representations of temporal-spatial data allows for the creation of a spatial-temporal variogram (Fig. 15.2) using the Product-Sum Model, applied to infrastructure lifeline system restoration in space and time. A given point on the surface of the spatial-temporal variogram can be interpreted as the restoration variance at a given spatial and temporal lag combination. Using a set of spatially-dependent, temporally-dependent, and spatial-temporal variograms on the data, the sills corresponding to each variogram are estimated using an exponential model variogram fit. For example, the spatial-temporal sill $C_{s,t}$ associated with the variogram shown in Fig. 15.2 is 0.1484. These values are used in the determination of the constants k_1, k_2, and k_3 according to Eqs. 15.12–15.14 to guarantee positive definiteness. The resulting spatial-temporal variogram offers a joint variability for every combination of lag in space and time.

Kriging is then applied using the spatial-temporal variogram by cutting the variogram surface such that spatial correlation or local interdependency can be observed in slices for each time lag. In order to calculate such local interdependencies, a local mesh of 101 points is constructed by kriging around each node for each system. Then, a correlation analysis can be performed between the water and power network local meshes (without relative displacements) for a given time, yielding a measure of local coupling strength in a particular service area. The Pearson's correlation values calculated for each node of the restoration surfaces are then kriged once again to depict the local distribution of correlation in the region per unit of time (Fig. 15.3). By translating the kriging restoration surfaces by a certain radial distance and angle (e.g., a radial mesh of 20 angle increments and 500 m radial increments up to 2,500 m away from evaluation nodes per restoration surface), the correlation of the restoration levels between the reference and adjunct networks can also be analyzed. Autocorrelation represents the dependency within the same network, while cross-correlation refers to the interdependency between different networks.

The shifting of one network surface from another reference network surface is performed not only for distinct lags in space but also time. The translations in time and space of the adjunct network surface will yield global correlation plots, which

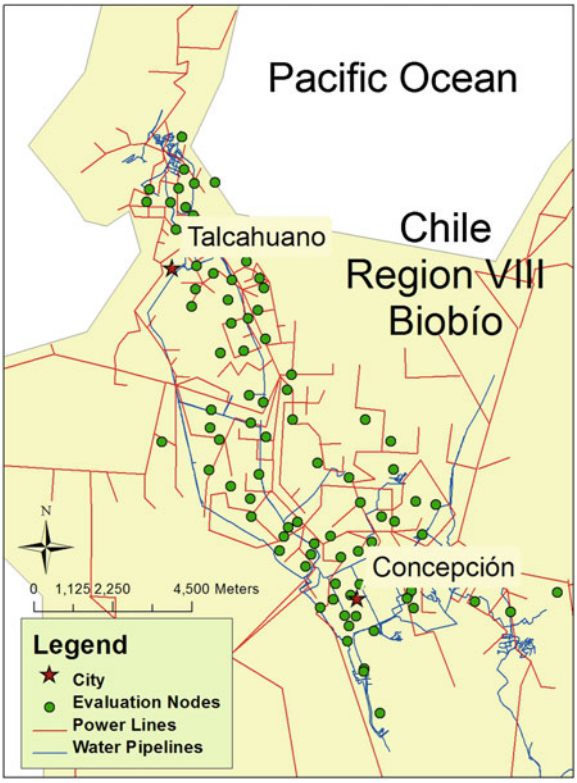

Fig. 15.1 Map of the evaluation nodes from the Talcahuano and Concepción region during the 2010 Chilean Earthquake along with streamlined transmission level power and water networks

can also be averaged to find overall interdependencies and their lengths of influence

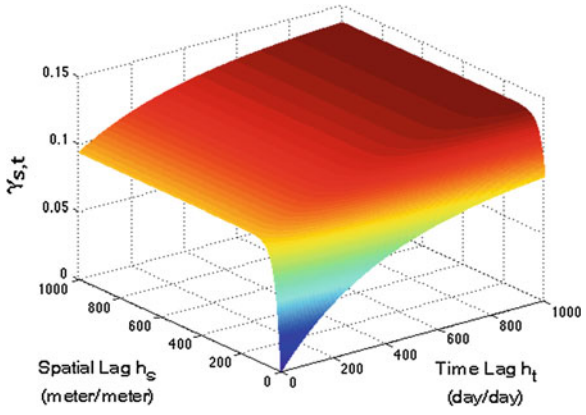

Fig. 15.2 The spatial-temporal variogram surface of the water system as a function of temporal and spatial lag normalized by the maximum value in each data set

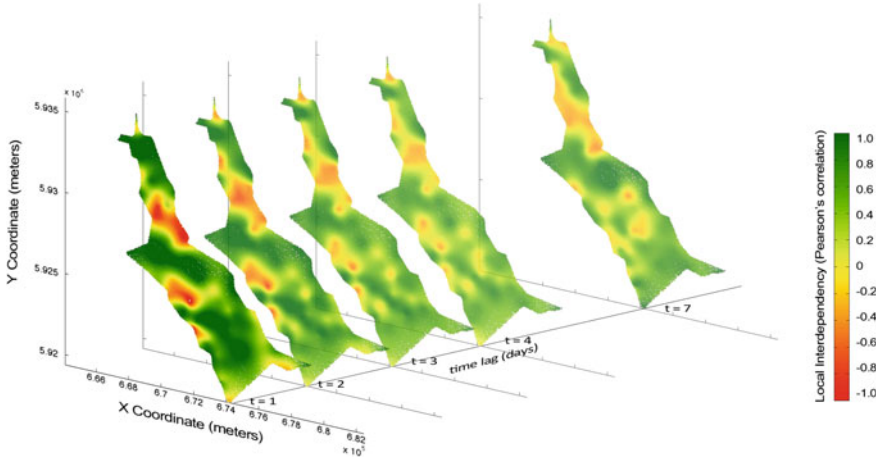

Fig. 15.3 Evolution of local interdependencies across space and time in the Talcahuano-Concepción region of Chile

as a function of time, as discussed in the next section. Note for now that Fig. 15.3 is the first depiction of interdependence evolution in time as a function of spatial location. The local correlation map highlights the richness and heterogeneity of the interdependencies, which differ from assumptions in early models of networks of networks that use homogeneous and static coupling strengths.

15.4 Analysis and Discussion of Synthesized Interdependencies

From the temporal evolution of the local correlations or interdependencies in the region (Fig. 15.3), it is possible to view a generalized summary of the spatial-temporal coupling between the power and water networks. What appears to be highly localized negatively or positively correlated regions in the map corresponds to local circumstances, demonstrating the spread of correlations across space, dependent upon the physical location of the networks, their state of damage, and adopted restoration strategies. The correlations of these areas are still evident through time, but the heterogeneity decreases as the time lag increases, verifying the intuitive result that correlation due to location diminishes as restoration levels of nodes reach higher and higher serviceability, thus reducing variability across them. After about a week after the earthquake event, there is a notable decrease in negative local correlations between the power and water systems, but as the majority nodes begin to reach full restoration, interdependencies are still visible although at reduced strengths.

Global correlation plots (Fig. 15.4) are created by displacing entire restoration surfaces relative to each other in space, so as to show spatial correlations in polar coordinates across time steps as a function radial distance and angle from

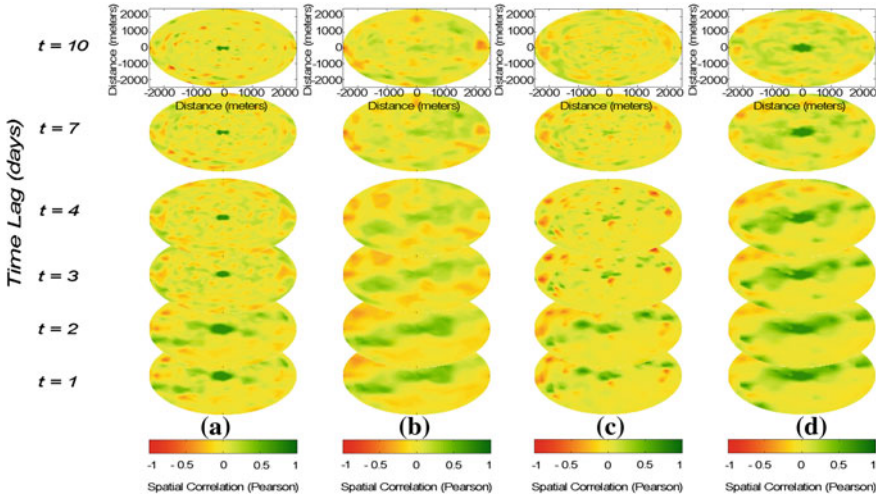

Fig. 15.4 Global correlation plots (with North taken in the upwards direction) synthesizing restoration surfaces between and across systems as a function of time as well as a function of radial distance and angle shown in four stacks depicting: (**a**) the power–power auto-correlation, (**b**) water-power cross-correlation (power as the reference network), (**c**) power-water cross-correlation (water as the reference network), and (**d**) the water–water auto-correlation

the shifted surfaces. The resulting polar-coordinate plots measure the global interdependence across translated maps and reveal the distance and direction in which interdependencies matter. The global correlation plots are presented in four stacks of adjunct-reference network pairs, depicting from left to right: the power–power auto-correlation, water-power cross-correlation (power as the reference network), power-water cross-correlation (water as the reference network), and the water–water auto-correlation. The auto-correlation plots start from a synthesized correlation of 1.0 at the center, since it intuitively represents the same network data. For all the plots, there are signs of directionality at earlier time steps, hinting at general correlations northeast or southwest of evaluation node sets. This may be due to the inherent shape of the analyzed region and associated networks, as well as the distribution of damage and the location of their main components [41]. However, traces of directionality are not evident as time lags increase. The two auto-correlations exhibit unique temporal trends, where the power auto-correlation moves from a central cluster of positive correlation to a relatively uncorrelated neighborhood, while the water network has a much larger neighborhood of high positive correlation that maintains directionality and a certain level of spatial correlation in all directions within a radial proximity of less than 500 m as time progresses. The auto-correlation of the water system (Fig. 15.4, Part d) shows the strongest directionality in recovery as the water system has a concentration of pumping stations and tanks, along with the main water treatment plant in the southwest to northeast direction. Cross-correlation plots are clearly anisotropic, particularly for large lag times, but reflect similar initial correlations

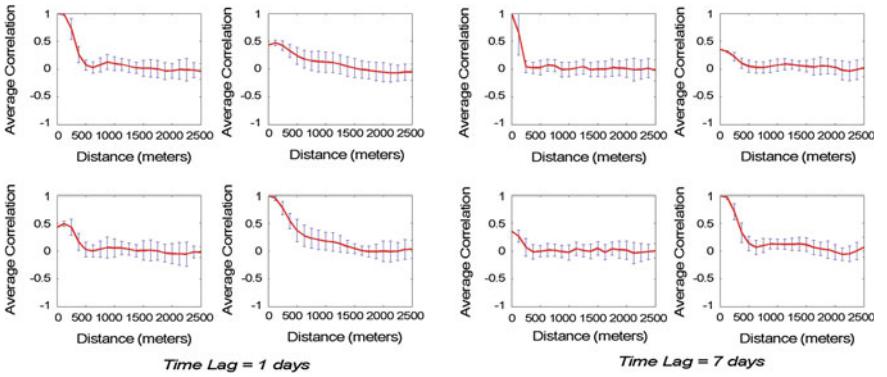

Fig. 15.5 Global interdependence plots of overall Pearson's correlation averaged over all angles as a function of radial distance at a time lag of 1 and 7 days. For each time lag, the plots are subdivided into four subplots depicting in a clockwise direction starting from the top left, the power–power auto-correlation, the water-power cross-correlation (power as the reference network), the water–water auto-correlation, and the power-water cross-correlation (water as the reference network)

with a diagonal trend of weak correlations northeast and southwest of the evaluation nodes, mainly contributed by the water system characteristics and the availability of electricity. At the same time, the trend is still stronger when the power system is taken as the reference system, highlighting a greater operational and logistical influence of the power system on the water system than vice versa. Overall, the global correlation plots provide an illustrative synthesis of the spatial interdependencies over time and reveal an inherent directionality in the infrastructure restoration trends which capitalize on alternative paths and follow directions perpendicular to the main axis of networks.

The overall correlation plots or average global interdependence plots (Fig. 15.5) further consolidate the data by averaging across all angles in Fig. 15.4 to obtain the average correlation for a given distance relative to the two displaced networks. The plots are compared at different points in time and include error bars indicating one standard deviation from the mean. For each time lag, the plots are subdivided into four interdependence plots depicting in a clockwise direction starting from the top left, the power–power auto-correlation, the water-power cross-correlation (power as the reference network), the water–water auto-correlation, and the power-water cross-correlation (water as the reference network). The off diagonal plots reveal the change in coupling strength between the power and water networks in the region. While initial cross correlations begin at under 0.5, it is evident that correlations exist up to approximately 2,000 m before reducing to almost zero at low time lags. Also, comparisons of the relationship between average correlation and distance from a time lag of 1 day to 7 days show a faster decay in correlation behavior with time. Plotting average global correlations versus distance over time can lead to the creation of surfaces that reflect the overall evolution of average coupling strengths between networks. While the average global interdependence plots allow for a succinct representation

of overall spatial trends of interdependencies, average plots may obscure trends that are evident in analyses of global or local interdependency, hence the need to jointly explore local, global and average global information for practical network of networks modeling and operation recommendations. Clearly, the geographically focused reach of interdependence effects offers insights into siting and timing of back-up resources to handle the propagation of interdependent cascades, as well as the sizing or capacity requirements of equipment and crews.

The spatial-temporal methodology presented in this chapter is shown to be applicable within the context of infrastructure network interdependency, and furthermore, takes into consideration factors traditionally unaccounted for such as time and space. The demonstrated approach highlights the multifaceted and evolving nature of infrastructure network interdependencies and allows for the depiction of heterogeneity of interdependence in space and its evolution in time. Insights from the analyses include the ability to reveal interdependence directionality as well as to identify and measure the length in which interdependence remains influential. The application of graphical and mathematical tools in the quantification of interdependence contributes to the better understanding of network coupling, and thus enables more comprehensive and accurate network of networks models to inform future design and mitigation actions. Knowledge of coupling strengths may lead to possibilities in the exploitation of interdependencies for efficient operations or the decoupling or reduction of network dependence during post-disaster or remediation periods.

At the same time, spatial-temporal analyses remain highly dependent on data availability as well as the reliable fitting of the space and time variograms. Limitations to the model include the assumptions inherent in the product-sum estimation model and the accuracy of the sill-dependent coefficients of the covariance function. While the global and average global correlation plots succinctly summarize general network dependency behaviors, they may over or underemphasize certain correlation aspects evident in local analysis, and thus motivate the need to study local interdependence plots as well. In the end, the spatial-temporal methodology can be used in conjunction with field observations and anecdotal data to support local to global trend interpretations. By comprehensively quantifying and understanding infrastructure coupling characteristics as well as informing theoretical and simulation-based multi-network models about interdependence, it is possible to ultimately capture inherent geographical and temporal interdependencies between critical infrastructure networks and exploit such properties to enhance operation, control, and restoration strategies.

15.5 Conclusions

Spatial-temporal analyses of network interdependencies are uncommon to complex infrastructure systems, thus the approach demonstrated in this chapter takes an important step towards understanding and quantifying the holistic relationships between networks of networks. Overall, this chapter serves to outline methodologies

used in analyzing interdependent networks and quantifying their coupling. Furthermore, a novel spatial-temporal approach is recommended to apply on infrastructure systems so as to reveal their coupling structure and inform models as well as practical design or mitigation recommendations. Utilizing previous efforts and developments in network theory and space-time methods, the approach presented in this chapter applies the Product-Sum method to quantify variability in interdependence in both time and space realms. In addition, analyzing through slices in time and space allows for the depiction of interdependence trends that exist in multiple dimensions so as to calibrate emerging models of networks of networks and to define future strategies for the control of interdependencies, including siting and staging of resources as well as strategies for interface decoupling.

A methodological application was provided with representations of power and water system restoration curves derived from the 2010 moment magnitude (M_W) 8.8 Chilean earthquake in the Talcahuano-Concepción region, resulting in the creation of a spatial-temporal variogram surface that served as the foundation for incorporating both time and space lag dependencies. Graphical depictions of interdependencies represented by Pearson's correlation coefficients revealed the heterogeneous nature of local infrastructure interdependencies and uncovered an inherent southwest to northeast directionality in the global plot of interdependencies when shifting network restoration maps. Finally, analyses from average global interdependency plots (overall correlations) demonstrated the changing radial extent of restoration correlation influence with time as a measure of coupling between networked systems which in some cases changed from 2.0 km to less than 0.5 km. These findings, enriched with global correlation plots and local coupling insights, imply that restoration is interdependent in the perpendicular direction of the studied systems, which highlights the need to ensure operation of the systems in their main direction through back-up systems of pertinent capacities or uncouplings of specific geographical extents related to the radial distances to which interdependencies matter.

Future research will include the creation of surface or volumetric representations of local correlation values in time and space to better track their evolution, and further build upon the understanding of interdependencies given spatial-temporal lags for different components and systems. At the same time, other spatial-temporal methodologies such as the graph wavelet-based approach will be studied for further research. This chapter provides a basic methodology and structure for quantifying spatial-temporal coupling across infrastructure networks and enables validation, calibration, and expansion of emerging interdependent infrastructure models. By demonstrating the applicability of spatial-temporal modeling among infrastructure networks, research and design in future complex network interdependence can yield more accurate and realistic results for protecting utility networks and their users, particularly after episodes of abnormal operation.

Acknowledgments The research in this chapter has been funded in part by the National Science Foundation (NSF) through the grant CMMI-0748231. Any opinions, findings, and conclusions or recommendations expressed in this material are those of the authors and do not necessarily reflect the views of the National Science Foundation.

References

1. Amin M (2001) Toward Self-Healing Infrastructure Systems. Computer Applications in Power, IEEE 14.1:20–28, doi:10.1109/67.893351
2. Barrat A, Boccaletti S, Caldarelli G, Chessa A, Latora V (2008) Complex Networks: from Biology to information technology. Journal of Physics A 41 220301
3. Barthélemy M. (2010) Spatial networks. ARXIV 2010arXiv1010.0302B.
4. Bashan A, Bartsch R, Kantelhardt J W, Havlin S, and Ivanov P (2012) Network physiology reveals relations between network topology and physiological function. Nature Communications 3.702, doi:10.1038/ncomms1705
5. Brummitt C, D'Souza R, and Leicht E (2012) Suppressing Cascades of Load in Interdependent Networks. PNAS 109.12:E680–E689, doi:10.1073/pnas.1110586109
6. Buldyrev S V, Parshani R, Paul G, Stanley H E, and Havlin S (2010) Catastrophic Cascade of Failures in Interdependent Networks. Nature 464:1025–1028
7. Chang S, McDaniels T, and Beaubien C (2009) Societal impacts of infrastructure failure interdependencies: building an empirical knowledge based. Proc. of the 2009 TCLEE Conference, Oakland, CA, 693-702
8. Clinton, W J (1996) Executive order 13010, establishing the president's commission on critical infrastructure protection (PCCIP), U.S.Government Printing Office, Washington, D.C.
9. Cressie N, Huang H (1999) Classes of Nonseparable, Spatio-temporal Stationary Covariance Functions. JASA 94:1330–1340
10. Crovella M, Kolaczyk E (2002) Graph Wavelets for Spatial Traffic Analysis. In IEEE INFOCOM
11. De Cesare L, Myers D, Posa D (2001) Estimating and modeling space-time correlation structures. Statistics and Probability Letters, 51.1:9–14
12. De Iaco S, Myers D, Posa D (2001) Spacetime analysis using a general productsum model, Statistics and Probability Letters. 52.1:21–28, doi:10.1016/S0167-7152(00)00200-5
13. Dueñas-Osorio L, Craig J, Goodno B, and Bostrom A (2007) Interdependent response of networked systems. Journal of Infrastructure Systems, 13.3: 185–194.
14. Dueñas-Osorio L, Craig J, and Goodno B (2007) Seismic response of critical independent networks. Earthquake Engineering and Structural Dynamics, 36.2: 285–306
15. Dueñas-Osorio L and Vemuru S M (2009) Cascading failures in complex infrastructure systems. Structural Safety, 31.2: 157–167
16. Dueñas-Osorio L, Kwasinski A (2012), Quantification of Lifeline System Interdependencies after the 27 February 2010 M_W 8.8 Offshore Maule, Chile, Earthquake. Earthquake Spectra 28.S1:S581–S603, doi:10.1193/1.4000054
17. Gao J, Buldyrev S V, Havlin S, and Stanley H E (2011) Robustness of a Network of Networks. Phys. Rev. Lett. 107, 195701
18. Gao J, Buldyrev S V, Havlin S, and Stanley H E (2012) Networks Formed from Interdependent Networks. Nature Physics 8:40–48
19. Gneiting T, Genton M, Guttorp P (2007) Geostatistical space-time models, stationarity, separability and full symmetry. In Statistical Methods for Spatio-Temporal Systems, Chapman and Hall/CRC, Boca Raton, 151–175.
20. Pidd H (2012) India blackouts leave 700 million without power. The Guardian. http://www.guardian.co.uk/world/2012/jul/31/india-blackout-electricity-power-cuts
21. Haimes Y and Jiang P (2001) Leontief-based Model of Risk in Complex Interconnected Infrastructures. Journal of Infrastructure Systems 7.1: 1–12
22. Havlin S (2009) Phone Infections. Science 324:1023–1024
23. Hernández-Fajardo I and Dueñas-Osorio L (2013). Probabilistic study of cascading failures in complex interdependent lifeline systems. Reliability Engineering and System Safety, 111: 260–272.
24. Kröger W (2008) Critical infrastructures at risk: A need for a new conceptual approach and extended analytical tools. Reliability Engineering and System Safety, 93.12:1781–1787, ISSN 0951–8320, doi:10.1016/j.ress.2008.03.005

25. Lee E, Mitchell J, and Wallace W (2007), Restoration of Services in Interdependent Infrastructure Systems: A Network Flows Approach, IEEE Transactions on Systems, Man, and Cybernetics Part C: Applications and Reviews 37:13031317
26. Mendonça D, Lee E E, and Wallace W A (2006) Impact of the 2001 World Trade Center Attack on Critical Interdependent Infrastructures. J. Infrastruct. Syst., 12.4: 260–270, doi:10.1061/(ASCE)1076-0342
27. Lee R and Kiremidjian A S (2007) Uncertainty and Correlation for Loss Assessment of Spatially Distributed Systems. Earthquake Spectra 23.4: 753–770.
28. Ouyang M and Dueñas-Osorio L (2011) Efficient Approach to Compute Generalized Interdependent Effects between Infrastructure Systems. J. Comput. Civ. Eng., 25.5:394–406, doi:10.1061/(ASCE)CP.1943-5487.0000103
29. Quill E (2012) When Networks Network: Once studied solo, systems display surprising behavior when they interact. Science News 182.6:18
30. President's Commission on Critical Infrastructure Protection (PCCIP). (1997). Critical foundations: Protecting Americas infrastructures. Rep., U.S. Government Printing Office, Washington, D.C.
31. Rahnamay-Naeini M, Pezoa J, et al. (2011) Modeling Stochastic Correlated Failures and their Effects on Network Reliability. Computer Communications and Networks (ICCCN), Proceedings of 20th International Conference on 1–6, doi:10.1109/ICCCN.2011.6005789
32. Rinaldi S, et al. (2001) Indentifying, understanding, and analyzing critical infrastructure interdependencies. IEEE Control Systems Magazine 21:11–25
33. Rosato V, Issacharoff L, Tiriticco F, and Meloni S (2008), Modeling interdependent infrastructures using interacting dynamical models. Int. J. Crit. Infrastruct., 4(1–2), 6379.
34. Satumtira G and Dueñas-Osorio L (2010). Chapter 1: Synthesis of modeling and simulation methods on critical infrastructure interdependencies research. Sustainable Infrastructure Systems: Simulation, Imaging, and Intelligent Engineering. Eds. K. Gopalakrishnan and S. Peeta. New York: Springer-Verlag.
35. Svendsen N K and Wolthusen S D (2007), Connectivity models of interdependency in mixed-type critical infrastructure networks. Inform. Sec. Tech. Rep., 12(1), 4455.
36. Sydney A, Scoglio C, Youssef M, Schumm P (2010), Characterizing the Robustness of Complex Networks. Int. J. Internet Technology and Secured, Transactions. 2.3/4:291–320
37. Technical Council on Lifeline Earthquake Engineering (TCLEE), (2010) Preliminary report on lifeline system performance after the M_W 8.8 offshore Maule, Chile, earthquake of February 27, 2010, American Society of Civil Engineers (ASCE)
38. Trauth M H (2010) MATLAB Recipes for Earth Sciences. Springer.
39. Sarma H and Russell R (2012) Second day of India's electricity outage hits 620 million. USA Today. http://usatoday30.usatoday.com/news/world/story/2012-07-31/india-power-outage/56600520/1
40. Wu J, Dueñas-Osorio L, and Villagran M (2012) Spatial Quantification of Lifeline System Interdependencies. Proceedings of the 15th world conference in earthquake engineering (15WCEE), Lisbon, Portugal, September 24–28, 2012
41. Wu J and Dueñas-Osorio L (2013) Calibration and validation of a seismic damage propagation model for interdependent infrastructure systems. Earthquake Spectra, 29.3:1021–1041
42. Zio E and Sansavini G (2011) Modeling Interdependent Network Systems for Identifying Cascade-Safe Operating Margins. Reliability, IEEE Transactions on 60.1:94–101, doi:10.1109/TR.2010.2104211